

LEWIS GRANT
IN 33-CR
286247
178.

ELECTRO-OPTIC NETWORK ANALYZER

Final Technical Report to the NASA Lewis Research Center

Contract #NCC 3-107

Dr. Todd A. Jackson

LABORATORY FOR LASER ENERGETICS

University of Rochester

250 East River Road

Rochester, NY 14623-1299

Date: 15 June 1990

(NASA-CR-186613) ELECTRO-OPTIC NETWORK
ANALYZER Final Technical Report (Rochester
Univ.) 17 p CSCL 09A

N91-14527

Unclas
G3/33 0286247

TABLE OF CONTENTS

I.	INTRODUCTION.....	3
II.	SAMPLING SYSTEM.....	6
III.	PHOTOCONDUCTIVE SWITCH GEOMETRY	9
IV.	SEMICONDUCTOR MATERIALS.....	10
V.	ION IMPLANTATION.....	11
VI.	EXPERIMENTAL RESULTS.....	12
VII.	REFERENCES	16

I. INTRODUCTION

The bandwidth of frequency-domain measurement techniques of electrical signals has typically been far greater than the bandwidth of time-domain methods. The primary limitations of the time-domain approach have been the 20–30 GHz bandwidth limit for electronic waveform acquisition instrumentation, and the lack of suitable electrical pulse generators for excitation of a test device. For this reason, network analysis has been performed using frequency-domain methods which, at present, yield the greatest measurement bandwidth, dynamic range, and sensitivity.

The bandwidth of frequency-domain network analysis appears to have reached a plateau of between 100 to 200 GHz, while time-domain measurements have improved markedly in both bandwidth and sensitivity recently with the introduction of the pulsed-laser based electro-optic sampling approach. Using this approach, electrical transients with millivolt amplitudes and subpicosecond rise times can be acquired. This ability equates to a measurement bandwidth in the hundreds of gigahertz, so that time-domain measurement techniques can now be applied to device characterization at high frequencies.

Network analysis, or, equivalently, the measurement of device scattering parameters (S-parameters) provides information necessary to the design of electronic networks such as high-frequency amplifiers, mixers, and phase-shifters. In the microwave and millimeter-wave frequency regimes, S-parameters are almost exclusively used for device characterization due to their many inherent advantages over other characterizing parameters. Compared to these other approaches, for example, S-parameters allow easier visualization and modeling of a circuit's behavior, regardless of its complexity.

The bandwidth of frequency-domain network analysis is, however, currently being exceeded by the newest generations of high-frequency transistors and devices. Thus the electro-optic approach is a natural means of extending network analysis into the range above 100 GHz by employing time domain methods. In this approach, a suitable electrical

excitation pulse is generated and propagated along a transmission line towards a test device that is to be characterized as shown in Fig. 1. At the electrical interface between the transmission line and device, the pulse is partially reflected with the reflected portion of the pulse's energy then propagating on the same transmission line but away from the device. The input reflection S-parameter describes the frequency dependence of the amplitude and phase relation between the sinusoidal components of these incident and reflected pulse waveforms. By acquiring these incident and reflected signals, the input reflection S-parameter (S_{11}) can be obtained.¹ For a one-port device, measurement of this single S-parameter comprises a complete characterization. To completely characterize a two-port device, however, three other S-parameters must be computed from additional waveforms obtained at other sample locations, and with excitation pulses applied to the output port of the device.

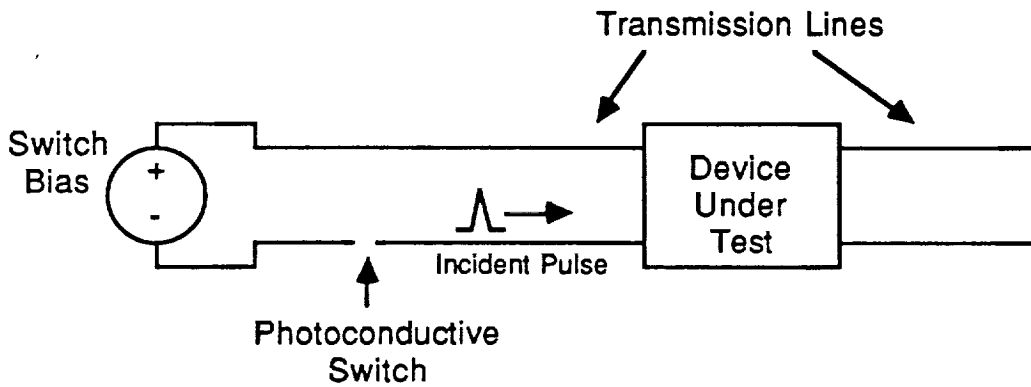


Fig. 1. Time-domain electro-optic network analyzer test fixture.

To elicit frequency-domain information such as S-parameters from acquired time-domain waveforms, Fourier transform or fast Fourier transform techniques must be employed. By computing the Fourier transform of an acquired waveform, the amplitude and phase of all sinusoidal components which comprise the signal are determined. Acquired waveforms which are to be Fourier transformed must, however, satisfy one

important criterion. The waveforms must be acquired without losing information about the waveshape through truncation, as the effect of truncation on the computed spectrum cannot be predicted or corrected for. In other words, both the excitation and reflected waveforms must be brief enough in duration to entirely fit within the sampling window of the waveform acquisition system. Developing the ability to generate short electrical pulses is thus an important step in the development of a time-domain electro-optic network analyzer.

In the picosecond domain, laser-driven photoconductive switches provide a unique method of generating electrical transients. Figure 2 shows a simple photoconductive switch that consists of metal electrodes deposited on a semiconductor with a gap of a few microns between the electrodes. This switch is closed by the optical generation of electron-hole pairs in the semiconductor material which allows a flow of charge to be induced from one electrode to the other by the application of an electrical bias applied across the electrodes. The electrical transient that is produced on the electrodes as a result of this charge transfer has a rise time that is dependent on both the optical excitation pulse rise time and the electrical time constant determined by the switch capacitance and electrode impedance. The duration of the electrical transient is largely determined by the carrier lifetime in the semiconductor.

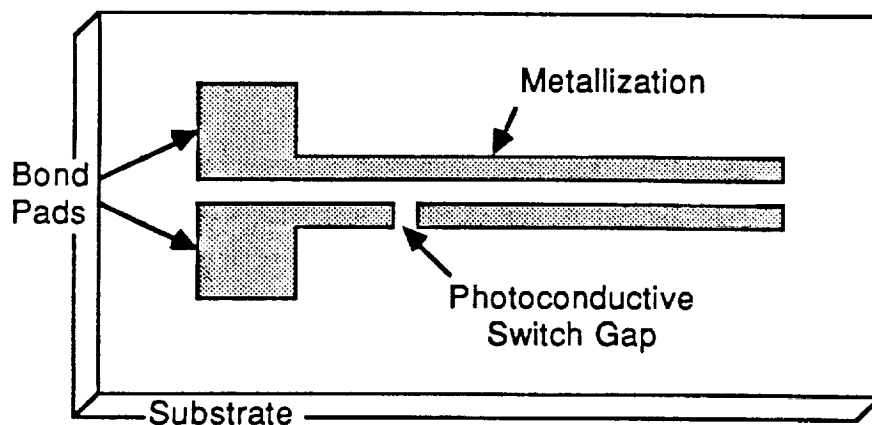


Fig. 2 Photoconductive switch geometry.

Photoconductive switches are required to produce pulses with durations of less than 10 ps, and with amplitudes up to 500 mV into a 50 Ω transmission line if they are to be employed in the area of device testing. During the course of this contract, we investigated several materials for generating short electrical pulses using photoconductive switches. This report describes the various semiconductor materials we tested for photoconductive switching, and the electro-optic measurement technique we used to characterize the material performance. *THE DESCRIPTION*

II. SAMPLING SYSTEM

Ultrafast sampling cannot be performed without a source of short optical pulses. The pulse laser employed in this research was a colliding-pulse, mode-locked (CPM) dye laser continuously pumped at 514 nm by an argon-ion laser. Figure 3 shows a schematic for this laser. The CPM laser emits two 100 MHz optical pulse-trains composed of pulses that are ~100 fs wide. Each pulse has, on average, 90 pJ of energy with a wavelength of ~620 nm, which is well suited for exciting photoconductive silicon and gallium-arsenide switches.

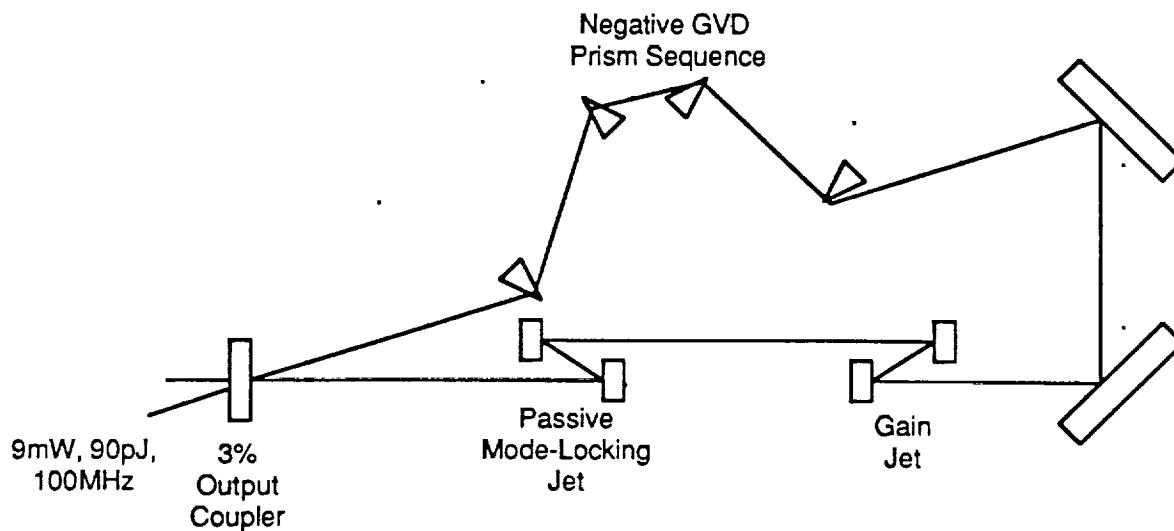


Fig. 3 CPM laser schematic.

The CPM laser produces short optical pulses through a passive mode-locking mechanism. The resonator, composed of a seven mirror ring cavity and cw-pumped rhodamine 590 gain medium, is mode-locked by the action of a DODCI absorber medium.² A four-prism sequence allows control of intracavity dispersion and enables optical pulses shorter than 100 fs to be produced.

The electro-optic sampling system is comprised of a lithium tantalate (LiTaO_3) electro-optic, total internal reflection (TIR) finger probe³ placed between crossed polarizers in a Pockels cell arrangement⁴ as shown in Fig. 4. In this system, one optical pulse train from the CPM laser is employed to excite the photoconductive switch to be tested, while the other beam synchronously samples the electric field-induced birefringence in the LiTaO_3 probe crystal. The change in the output of the slow detector, which measures the output of the Pockels cell, is proportional to the voltage on the transmission line at the sampling moment. Since the electro-optic sampling system employs the same laser for waveform sampling as for exciting the photoconductive switch, electrical waveforms are produced in precise temporal relation to the waveform sampling pulses. This reduces the sampling system jitter to well below 100 fs, yielding the high bandwidth inherent in this approach.

As demonstrated in Fig. 5, the TIR finger probe is "dipped" into the fringing field lines above the coplanar transmission line driven by the photoconductive switch and detects the fringing field of the electrical pulse as it propagates past the probe tip. The probe tip has the appearance of a flat-topped pyramid with a 40- μm square top. This extremely small physical dimension ensures that the finger probe does not dielectrically load the circuit and thus has a minimal effect on an propagating waveform. Before passing through the TIR probe, the sampling optical beam is sent through a variable delay rail, which allows the arrival time of sampling pulse to be swept across a wide time interval relative to the time when the photoconductive switch is excited. In this way, the sample pulse can be swept

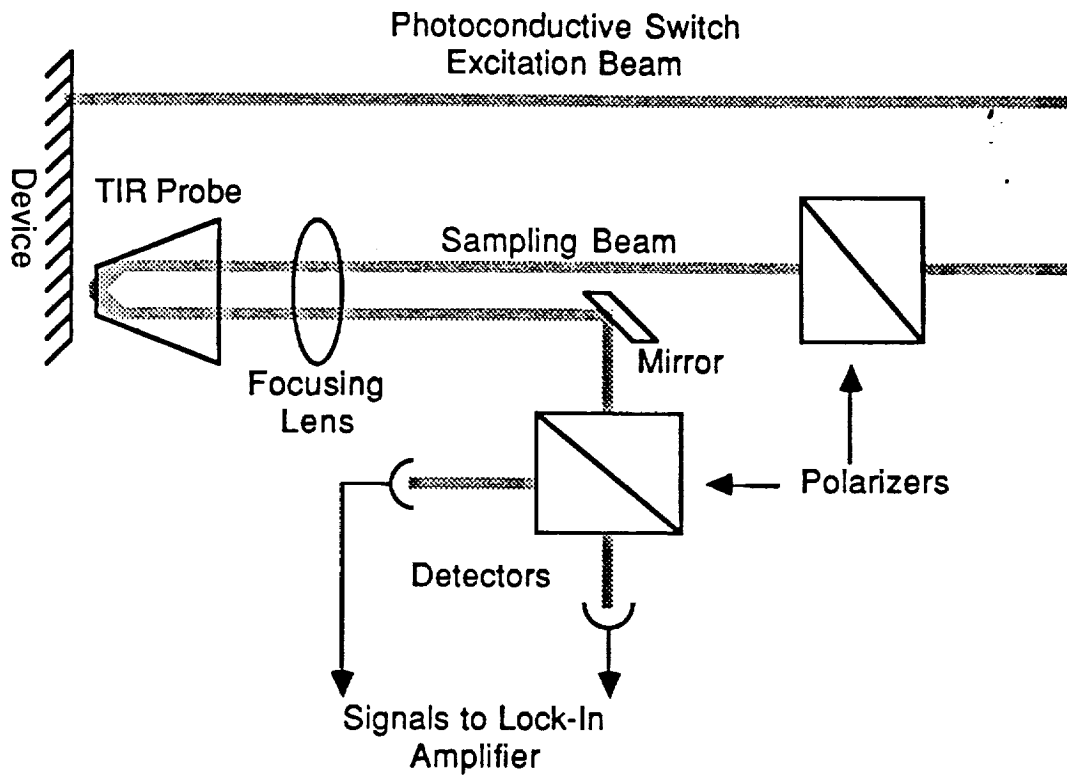


Fig. 4 TIR finger probe electro-optic sampling apparatus.

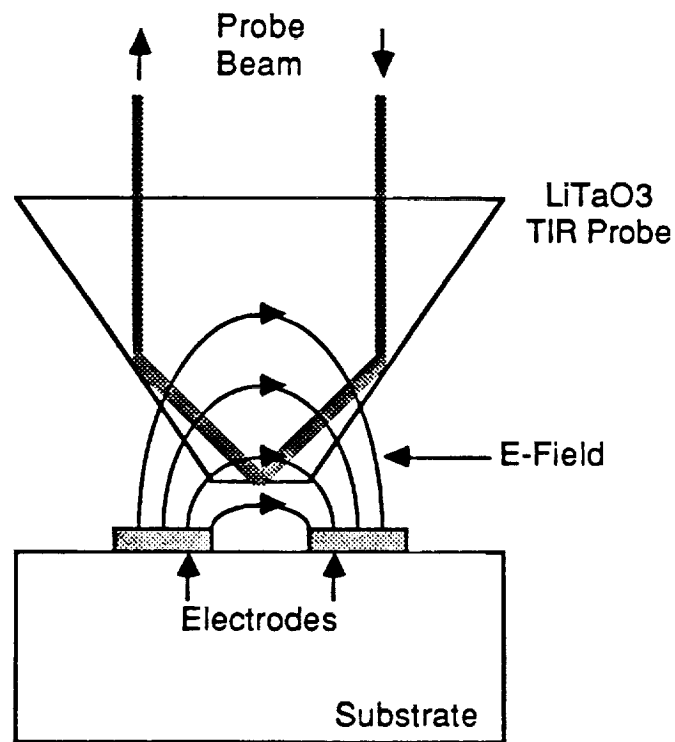


Fig. 5 TIR probe geometry.

across the electrical waveform produced by the switch, thereby allowing waveform acquisition.

As shown in Fig. 6, a lock-in amplifier is employed to improve the signal-to-noise ratio of the sampling system. Rather than applying a dc bias to the photoconductive switch, a square-wave bias is applied to modulate the switch operation on and off at a high frequency. The lock-in amplifier is then utilized to demodulate the acquired signal obtained from the Pockels cell. The signal-to-noise ratio of the sampling system is greatly improved when the modulating frequency is located at a low point in the laser noise envelope. For our CPM laser, best results were obtained by modulating at 3.95 MHz.

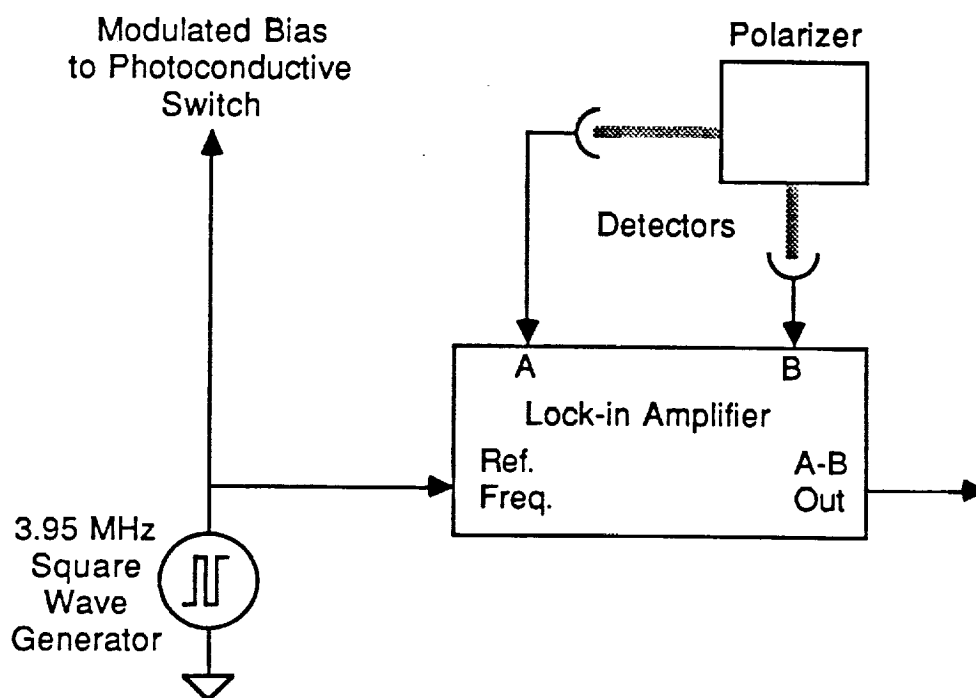


Fig. 6 High-frequency lock-in amplifier.

III. PHOTOCONDUCTIVE SWITCH GEOMETRY

To produce photoconductive switches, electrodes may be deposited on semiconductor materials in many geometries such as microstrip and coplanar strip line. For

the purpose of producing pulses in a way that is compatible for coupling them onto planar circuits and devices, we selected a coplanar electrode arrangement fashioned as an in-line switch in either the center conductor of a coplanar waveguide, or one conductor of a coplanar strip line as shown in Fig. 7. While electrical transients can be produced that are relatively insensitive to the position of the excitation beam on the switch through the use of interdigitated switches, the greater capacitance of these switches reduces the rise time of the electrical pulse produced, and a corresponding reduction in the high-frequency end of its amplitude spectrum occurs.⁵ Since high-frequency testing relies on a significant high-frequency spectral content, a straight gap was employed for all photoconductive switches.

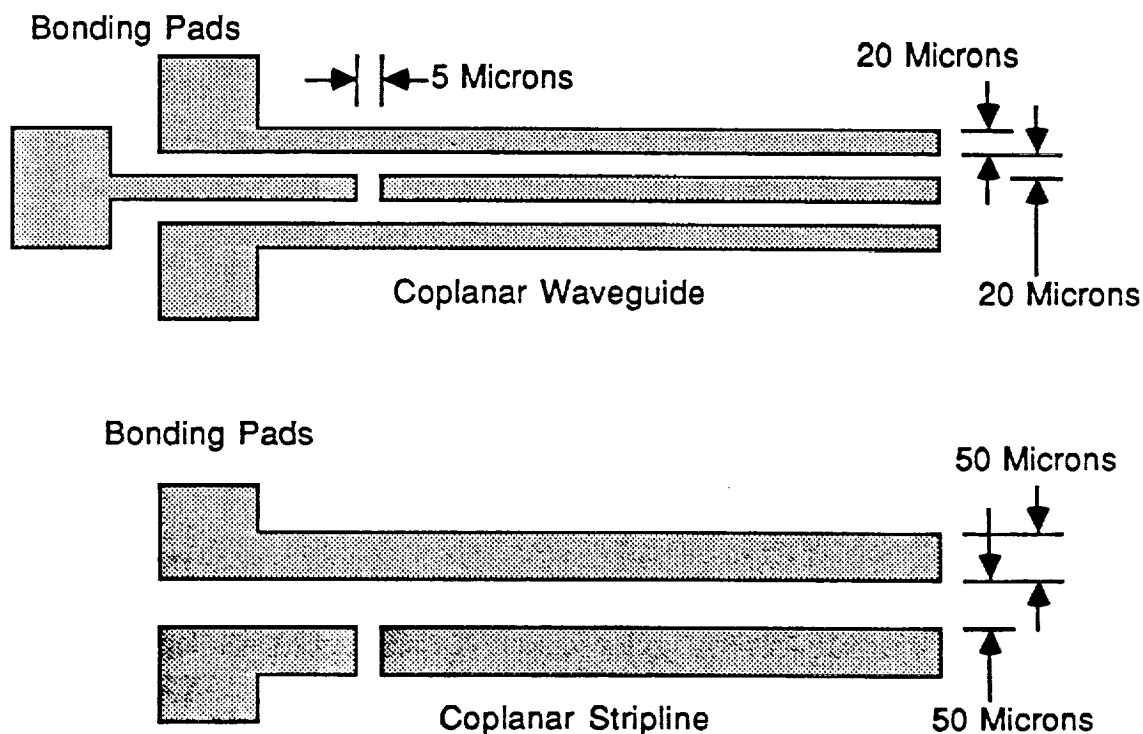


Fig. 7 Coplanar switch geometries.

IV. SEMICONDUCTOR MATERIALS

Many materials have been employed to produce electrical transients on coplanar transmission lines.^{6,7,8} Of these materials, Silicon (Si) and Gallium Arsenide (GaAs) are, perhaps, the most common substrates used in the manufacture of most electronic devices.

The utilization of a switch material compatible with commercial device substrates would allow integrated switches to be fabricated as part of a device metalization layer. In addition, the current generation of high-speed devices is commonly fabricated on GaAs substrates. For this reason we have limited the scope of our investigation of photoconductive switches to GaAs substrate materials.

V. ION IMPLANTATION

The electrical transient produced by a photoconductive switch excited by a 100-fs laser pulse has a duration that is predominantly dependent on the carrier lifetime in the substrate material. For both SOS and semi-insulating GaAs, the carrier lifetime is too long to be usable for producing the picosecond pulses required for high-frequency device testing. The GaAs switches, for example, produced pulses such as the one shown in Fig. 8 that were >300 ps in duration. An alternative approach to generating short pulses with photoconductive switches was thus required.

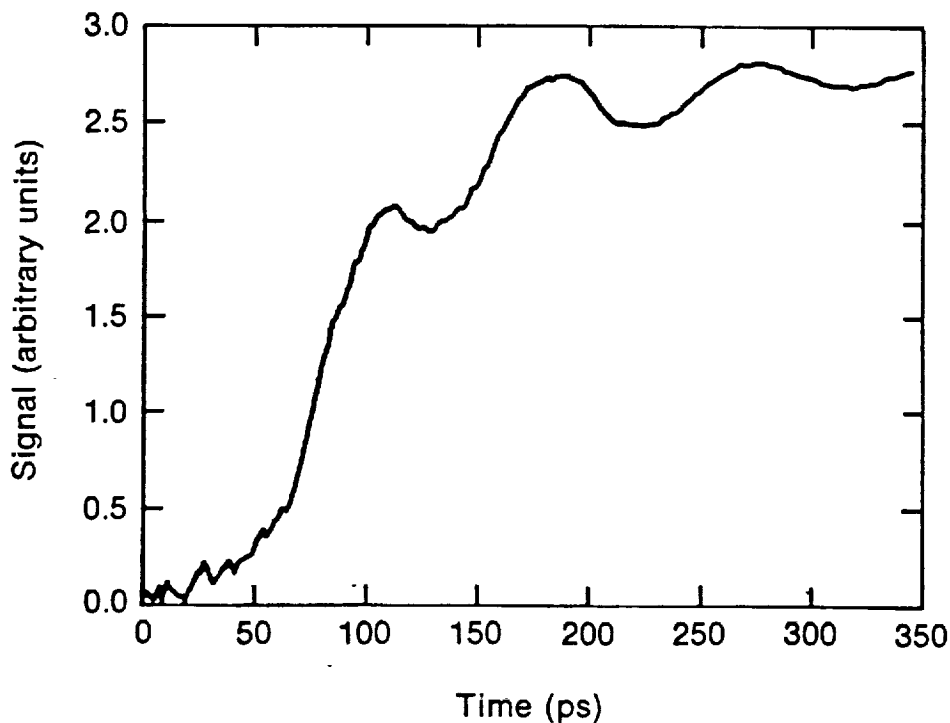


Fig. 8 Semi-insulating GaAs switch response.

Several investigators report success in reducing the carrier lifetime in both SOS and GaAs through the use of ion-implantation.^{7,8,9} The effect of ion-implantation is to create defects in the substrate material which serve as sites for carriers to be trapped and to recombine.

We tested coplanar strip line geometry GaAs switches damaged with four different proton (H^+) implant levels ranging from 1×10^{12} to $3 \times 10^{14}/\text{cm}^2$. The GaAs wafers used were 2 in. diam., <100> cut, 15 m thick, undoped, semi-insulating wafers implanted at doses of 1×10^{12} , 1×10^{13} , 1×10^{14} , and $3 \times 10^{14}/\text{cm}^2$. The implantation was performed at an energy of 100 keV to limit the implantation depth to less than $1 \mu\text{m}$.¹⁰ Implantation beyond $1 \mu\text{m}$ would not offer an advantage as the absorption depth for the 620-nm light from the CPM laser is $<1 \mu\text{m}$ and all electron-hole pairs will be produced within this depth. The wafers were uniformly implanted prior to the deposition of the metal electrodes. The electrodes were formed by thermal evaporation of 1000 Å of AuGe followed by 200 Å of Ni, capped by 1000 Å of AuGe to form a good ohmic electrode to semiconductor contact.

VI. EXPERIMENTAL RESULTS

A very low switching efficiency was observed from all switches implanted as described in the preceding section. In the case of the 1×10^{14} and $3 \times 10^{14}/\text{cm}^2$ implants, no output pulse could be observed at all. The explanation for this phenomenon is that although the carrier lifetime in the GaAs substrate is reduced through ion implantation, the mobility of the GaAs is also reduced as a consequence of the damage done to the crystal lattice by the implantation.⁸ In addition, since the damage extends across the entire substrate, the mobility in the substrate under the electrodes is also reduced. Since this portion of the material is never illuminated by the laser, no electron-hole pairs are produced under the electrodes, and the path for charge transfer across the switch gap is from the edge of one electrode in contact with the illuminated portion of the substrate to the edge of the

other electrode. This resulted in a low switch conductivity and consequent low switching efficiency.

An improved approach to ion implantation is to deposit the electrodes prior to implantation. In this case, ion implantation of the wafer surface covered by the metal electrodes is prevented by the metal. We tested a GaAs switch implanted with a dose of $1 \times 10^{13}/\text{cm}^2$ protons following the deposition of the coplanar waveguide metalization pattern pictured in Fig. 7. A typical electrical transient acquired 1 mm away from the switch on the coplanar waveguide is shown in Fig. 9. From this plot, the carrier lifetime time constant (τ) can be computed to be 29 ps. The switching efficiency, computed as the ratio of the peak value of the generated pulse to the peak value of the bias applied to the switch is $(0.0764/10)100\% = 0.764\%$.

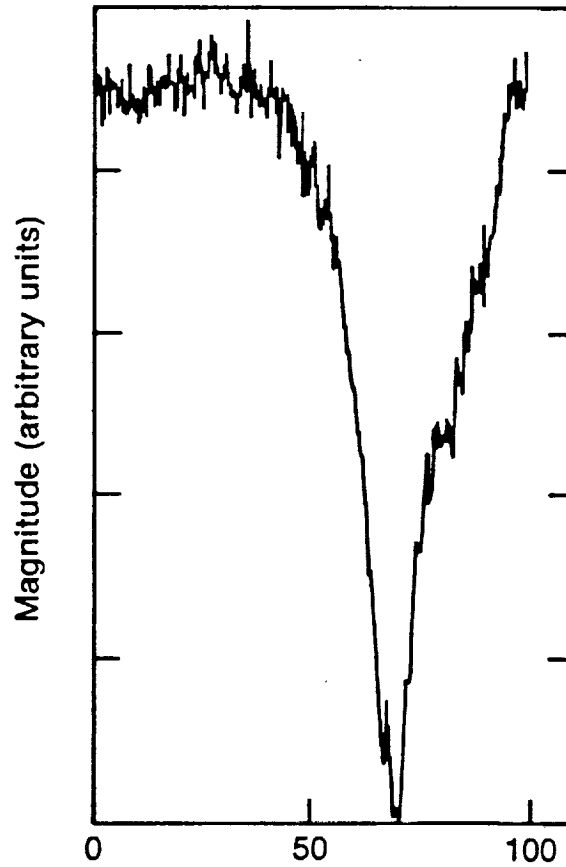


Fig. 9 Response of $1 \times 10^{13} \text{ H}^+$ implanted GaAs.

The observed pulse at this $1 \times 10^{13}/\text{cm}^2$ implantation dose is in agreement with that observed by Hammond,⁷ but we feel that a pulse of this duration is somewhat lengthy for use as an excitation pulse for high-frequency device testing. As a consequence, we anticipate that a higher implant dose must be employed to reduce the pulse width to the desired 10-ps duration. Increasing the implant dose to achieve this will, however, reduce the switching efficiency to an even lower value. Thus, for example, a switch with a 10- μm gap, which is able to withstand a bias voltage of about 10-V peak, will only produce a peak pulse voltage of <76 mV. A 10-ps pulse of this amplitude on a 50- Ω transmission line would have less than 6×10^{-19} J of energy. As this is quite far from the energy levels a general time-domain test system will be required to produce, we looked to other GaAs materials for short-pulse generation.

A novel GaAs material fabricated at MIT Lincoln Labs was then employed for photoconductive switching. This material was deposited by molecular beam epitaxy at 200°C using Ga and As₄ beam fluxes at a rate of 1 $\mu\text{m/hr}$ under arsenic stable growth conditions. As reported by the developers of this material,¹¹ this low-temperature GaAs (LT GaAs) is highly nonstoichiometric being composed of approximately 50.0% As and 49.5% Ga. The material tested consisted of a 2- μm layer of LT GaAs deposited at 200°C on a standard semi-insulating GaAs substrate.

The photoconductive switch geometry was that of a coplanar strip line with NiAuGe electrodes. A typical pulse measured at a distance of 100 μm from the switch for this material is shown in Fig. 10. The pulse width is ~ 1.6 ps with an amplitude of 300 mV.

We have shown that, with the proper substrate material, short-duration high-amplitude electrical pulses can be obtained from laser excited photoconductive switches. The combination of 6% switching efficiency, fast response, and compatibility with existing GaAs fabrication processes make LT GaAs ideal for time-domain studies of device

response, and for eventual incorporation into an electro-optic network analyzer. Many avenues of device testing such as picosecond characterization of transmission lines have been opened by the availability of this material. These investigations are beyond the scope of this investigation; however, at this point, we have obtained the necessary pulse-generating capability required to pursue time-domain studies of high-frequency devices.

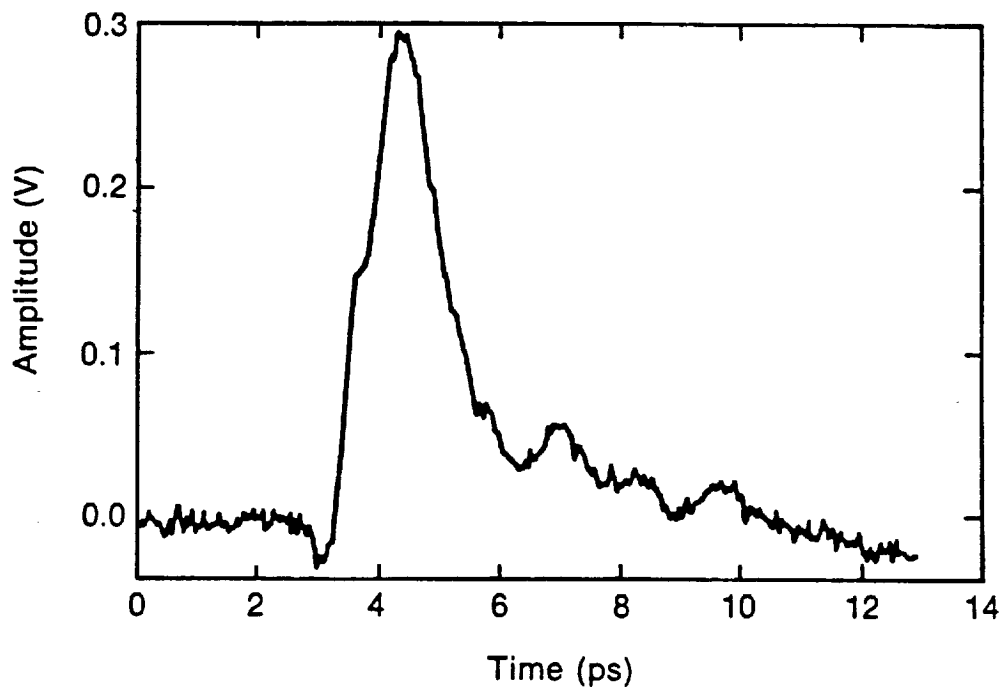


Fig. 10 Low-temperature GaAs switch response.

VII. REFERENCES

1. W. L. Gans and J. R. Andrews, "Time Domain Automatic Network Analyzer for Measurement of RF and Microwave Components," Electromagnetics Division, NBS, Boulder, CO, September, 1975.
2. J. A. Valdmanis and R. L. Fork, "Design Considerations for a Femtosecond Pulse Laser Balancing Self Phase Modulation, Group Velocity Dispersion, Saturable Absorption, and Saturable Gain," IEEE J. Quantum Electron. **OE-22** (1986).
3. J. Nees and G. Mourou, "A Total Internal Reflection (TIR) Finger Probe for Electro-Optic Sampling," Electron. Lett. **32**, 918 (1986).
4. J. A. Valdmanis and G. Mourou, "Subpicosecond Electro-optic Sampling: Principles and Applications," IEEE J. Quantum Electron. **OE-22** (1986).
5. D. H. Auston, "Impulse Response of Photoconductors in Transmission Lines," IEEE J. Quantum Electron. **OE-19** (1983).
6. M. C. Nuss, D. W. Kisker, P. R. Smith, and T. E. Harvey, "Efficient Generation of 480-fs Electrical Pulses on Transmission Lines by Photoconductive Switching in MOCVD-CdTe," (preprint).
7. R. B. Hammond, N. G. Pauliter, and R. S. Wagner, "Observed Circuit Limits to Time Resolution in Correlation Measurements with Si-on-sapphire, GaAs, and InP Picosecond Photoconductors," Appl. Phys. Lett. **45**, 1 (1984).
8. P. Polak-Dingels, G. Burdge, Chi H. Lee, A. C. Seabaugh, R. T. Brundage, M. I. Bell, and J. Albers, "An Investigation of Photoconductive Picosecond Microstripline Switches on Self-Implanted Silicon on Sapphire (SOS)," Picosecond Electronics and Optoelectronics II: Proc. of the Second OSA-IEEE (LEOS), Incline Village, Nevada, 14-16 January 1987, pp. 232-235.

9. F. E. Doany, D. Grischkowsky, and C.-C. Chi, "Carrier Lifetime Dependence on Ion Implantation in Silicon, Picosecond Electronics and Optoelectronics II: Proc. of the Second OSA-IEEE (LEOS), Incline Village, Nevada, 14–16 January 1987, pp. 228–231.
10. K. Steeples and I. Saunders, "Damage Ranges for Implanted Hydrogen Isotopes in Gallium Arsenide," IEEE Trans. Nucl. Sci. **NS-30** (1983).
11. S. Gupta, J. A. Valdmanis, G. A. Mourou, F. W. Smith, and A. R. Calawa, "Single Picosecond Pulse Generation in Low Temperature MBE Grown GaAs Photoconductors," Conference on Lasers and Electro-Optics (CLEO), Baltimore, MD, 24–28 April 1989.